Epigenetic Changes in Mitochondrial Superoxide Dismutase in the Retina and the Development of Diabetic Retinopathy

Qing Zhong and Renu A. Kowluru

OBJECTIVE—To investigate the role of epigenetic regulation of the manganese superoxide dismutase gene (*sod2*) in the development of diabetic retinopathy and the metabolic memory phenomenon associated with its continued progression after hyperglycemia is terminated.

RESEARCH DESIGN AND METHODS—Streptozotocin-induced diabetic rats were maintained in poor glycemic control (PC, GHb ~12%) or in good glycemic control (GC, GHb ~7.0%) for 4 months, or were allowed to maintain PC for 2 months, followed by GC for 2 additional months (PC-Rev). For experimental galactosemia, a group of normal rats were fed a 30% galactose diet for 4 months or for 2 months, followed by a normal diet for 2 additional months. Trimethyl histone H4 lysine 20 (H4K20me3), acetyl histone H3 lysine 9 (H3K9), and nuclear transcriptional factor NF-κB p65 and p50 at the retinal *sod2* promoter and enhancer were examined by chromatin immunoprecipitation.

RESULTS—Hyperglycemia (diabetes or galactosemia) increased H4K20me3, acetyl H3K9, and NF-κB p65 at the promoter and enhancer of retinal *sod2*, upregulated protein and gene expression of *SUV420h2*, and increased the interactions of acetyl H3K9 and NF-κB p65 to H4K20me3. Reversal of hyperglycemia failed to prevent increases in H4K20me3, acetyl H3K9, and NF-κB p65 at *sod2*, and *sod2* and *SUV420h2* continued to be abnormal. Silencing *SUV420h2* by its small interfering RNA in retinal endothelial cells prevented a glucose-induced increase in H4K20me3 at the *sod2* enhancer and a decrease in *sod2* transcripts.

CONCLUSIONS—Increased H4K20me3 at *sod2* contributes to its downregulation and is important in the development of diabetic retinopathy and in the metabolic memory phenomenon. Targeting epigenetic changes may serve as potential therapeutic targets to retard the development and progression of diabetic retinopathy. ***Diabetes*** **60:1304–1313, 2011**

Retinopathy is a debilitating vascular complication of diabetes. Despite extensive research, the molecular mechanism of its development remains elusive. Superoxide radicals are elevated in the retinal mitochondria and their scavenging enzyme, manganese superoxide dismutase (MnSOD), is compromised (1–3). This decrease in MnSOD activity is observed as early as 2 months after induction of hyperglycemia in rats (1), and the enzyme remains compromised at duration when capillary cell apoptosis or pathology characteristic of diabetic retinopathy are observed in the retinal vasculature (4–7). Prevention of MnSOD inhibition by the administration of antioxidants or overexpression of *sod2* prevents the development of diabetic retinopathy in rodents (6,8,9), suggesting it has a major role in the development of diabetic retinopathy. However, how diabetes regulates retinal MnSOD remains to be explored.

The nuclear gene, *sod2*, encodes MnSOD, and the transcription of *sod2* is driven by regulators binding on its promoter and enhancer regions (10,11). Redox-sensitive nuclear transcriptional factor, NF-κB, which acts as pro-apoptotic factor in the pathogenesis of diabetic retinopathy, binds to the promoter and enhancer of *sod2*. The NF-κB p65/p50 heterodimer increases *sod2*, and p50/p50 suppresses it (12–14). Gene expression is also regulated by the chromatin structure that is modulated by histone modifications (15). Acetylation of histone H3 lysine 9 (H3K9) is considered to activate gene transcription, and trimethylation of histone H4 lysine 20 (H4K20) to repress (15). These modifications are initiated by specific enzymes, and SUV420h2/KMT5C (SUV420h2) is considered one of the prime enzymes for the trimethylation of H4K20 (16). High glucose exposure of bovine aortic endothelial cells altered methylation of H3K4 and H3K9 on the p65 promoter of NF-κB (17). However, regulation of retinal *sod2* in diabetes by histone modifications and NF-κB remains unclear.

Good glycemic control, if started in the initial stage of diabetes, prevents the development of retinopathy, but if reinstituted after a period of poor control, fails to halt its development, suggesting a metabolic memory phenomenon. Patients in the conventional treatment regimen during the Diabetes Complications and Control Trial had a higher incidence of complications several years after switching to intensive therapy than the patients in intensive control (18). Studies in rats have demonstrated that the retina continues to experience oxidative stress, MnSOD remains compromised, and NF-κB is activated for at least 6 months after reinstitution of good glycemic control that has followed 6 months of poor control (7,19–21). The accumulation of damaged mitochondrial DNA continues in the retina and its capillary cells (22,23). Histone modifications are linked with persistent activation of NF-κB after transient hyperglycemia in aortic endothelial cells, and this activation is prevented by reducing mitochondrial superoxide (24). Our recent study has suggested the role of retinal H3 global acetylation in the metabolic memory phenomenon (25). However, how the epigenetic regulation of *sod2* contributes to the metabolic memory phenomenon remains to be explored.

In the current study, we used two animal models of diabetic retinopathy to investigate the mechanism by which histone modifications regulate retinal *sod2* in the development of retinopathy and in the metabolic memory

From the Kresge Eye Institute, Wayne State University, Detroit, Michigan.
Corresponding author: Renu A. Kowluru, rkowluru@med.wayne.edu.
Received 26 January 2010 and accepted 27 January 2011.
DOI: 10.2337/db10-0133

phenomenon associated with its resistance to arrest after hyperglycemia is terminated. Because the retina is a complex tissue with multiple cell types, key findings are also confirmed in isolated retinal endothelial cells, the cells that are the target of the histopathology that is characteristic of diabetic retinopathy.

RESEARCH DESIGN AND METHODS

Animals. Wistar rats (male, 200 g) were randomly assigned to normal, diabetic, or experimentally galactosemic groups. Diabetes was induced with streptozotocin (55 mg/kg body wt), and 3 to 4 days after induction of diabetes, the rats were divided into three groups: group 1 rats were in poor glycemic control (glycated hemoglobin [GHb] >12%) for 4 months (PC group), group 2 rats were in poor control for 2 months, followed by good control for 2 additional months (PC-Rev group), and group 3 rats were in good control (GC group, GHb ~7.0%). The PC rats received 1 to 2 units of insulin (Humulin; Eli Lilly, Indianapolis, IN) four to five times a week, and the GC rats received insulin twice daily for a total of 7 to 8 units. Experimental galactosemia was induced in normal rats (Galac group) by feeding 30% galactose supplemented diet. The Galac group rats received the galactose diet for the entire 4 months of the study, and the Galac-Rev group received galactose diet for the first 2 months and a normal diet for 2 additional months. The control group comprised normal age-matched rats.

Blood was obtained by weekly tail vein puncture to measure glucose by Freestyle Glucometer (Bayer, Tarrytown, NY), and GHb (every 2 months) using a kit from Helena Laboratories (Beaumont, TX). These procedures conformed to the Association for Research in Vision and Ophthalmology Resolution on Treatment of Animals in Research and are routinely used in our laboratory (7,12,19–22). At the end of the experiment, rats were killed by carbon dioxide asphyxiation, and the retina was removed immediately. About 50% of the retina was crosslinked with 1% paraformaldehyde, and the remaining was stored in liquid nitrogen.

Retinal endothelial cells and transfection. Endothelial cells prepared from bovine retina were cultured in medium consisting of 15% FBS (heat inactivated), 5% replacement serum (Nu-serum; BD Bioscience, San Jose, CA), heparin (50 μg/mL), endothelial growth supplement (25 μg/mL), and antibiotic/antimycotic in Dulbecco's modified Eagle's medium (9,23). Confluent cells from passages four to five were incubated in high glucose (20 mmol/L) for 4 days, followed by normal glucose (5 mmol/L) for 4 additional days (20-5 group). The controls included cells incubated in normal or high glucose for 8 days of the experiment, and 20 mmol/L mannitol served as an osmotic control. At the end of the incubation, the cells were processed for chromatin immunoprecipitation, as described below.

Endothelial cells from the passages three to five were transfected with small interfering RNA (siRNA) of *SUV420h2* or NF-κB p65 using transfection reagents from Santa Cruz Biotechnology (Santa Cruz, CA) as routinely performed in our laboratory (26). Briefly, after incubation of siRNA transfection complex for 45 min at room temperature, the cells were incubated with the transfection complex for 8 h at 37°C. Parallel incubations were done using nontargeting scrambled RNA. For *sod2* overexpression, the cells were incubated with 3 μg of *sod2* plasmid and effectene transfection reagent (Qiagen, Valencia, CA), as described by us (23). At the end of the transfection, the cells were washed with PBS and incubated in 5 mmol/L or 20 mmol/L glucose for 4 days. The transfection efficiency was verified by semiquantitative PCR using control primers from Santa Cruz Biotechnology.

Chromatin immunoprecipitation. Rat retina or isolated endothelial cells were crosslinked with 1% paraformaldehyde for 15 min. The fixed sample was resuspended in lysis buffer containing 1% SDS, 10 mmol/L EDTA, 50 mmol/L Tris-HCl, pH 8.1 (ChIP Assay Kit, Millipore, Temecula, CA), and protease inhibitor cocktail (Sigma-Aldrich, St. Louis, MO), and sonicated four to six times for 10 s each. Supernatant was diluted in ChIP dilution buffer containing 0.01% SDS, 1.1% Triton X-100, 1.2 mmol/L EDTA, 16.7 mmol/L Tris-HCl, pH 8.1, and 167 mmol/L NaCl, and precleared with protein A agarose/salmon sperm DNA for 30 min.

After a small aliquot of protein-DNA complex (15–20 μg) was collected for starting chromatin input, the protein-DNA complex was immunoprecipitated with the antibody against NF-κB p65 or p50, acetyl H3K9, H4K20me3 or rabbit normal IgG (Abcam, Cambridge, MA), or anti-general transcription factor IIB (TFIIB, Millipore Corporation, Temecula, CA). The immunoprecipitate collected with protein A agarose/salmon sperm DNA was washed sequentially with low-salt buffer, high-salt buffer, and LiCl buffer, according to the vendor's protocol. After the immunoprecipitate was washed twice with Tris-EDTA buffer, the sample was used for Western blotting or was extracted twice with 1% SDS containing 0.1 mol/L $NaHCO_3$.

Elutes and input were heated at 65°C for 4 h to reverse the formaldehyde crosslinking and digested with protease K at 45°C for 1 h. DNA fragments were recovered by phenol-chloroform-isoamyl alcohol extraction and ethanol precipitation, and resuspended in 20 μL water for PCR. Gene expression of *sod2* promoter and enhancer were quantified by SYBR green-based real-time quantitative PCR (q-PCR). Promoter of β-actin occupied by TFIIB and the off-target region of *sod2* were used as ChIP positive and negative controls, respectively, and normal rabbit IgG was used as the negative antibody control and DNA from input as the internal control. Each ChIP measurement was made in five to six rats per group or four to five cell preparations.

Gene expression. Gene expressions were confirmed by q-PCR using 7500 Real Time PCR System (Applied Biosystem, Foster City, CA) with SYBR green Master Mix (Applied Biosystem, Branchburg, NJ) or TaqMan primers.

Amplification of the *sod2* promoter and enhancer was performed in 1 μL of ChIP-purified DNA using the primers provided in Table 1. PCR was performed by denaturing at 95°C for 10 min, followed by 40 cycles of denaturation at 95°C for 15 s, annealing and extension at 60°C for 60 s, and this was followed by 95°C for 15 s, 60°C for 60 s, 95°C for 15 s, and 60°C for 15 s. The q-PCR values in

TABLE 1
PCR primers

	Primer sequence	Position
Rat *sod2* promoter		
Forward	CCAGGAATGGAAAAGGAGTG	−529 to −510
Reverse	CTTGTAACAGAGCGGCACAC	−282 to −301
Rat *sod2* enhancer		
Forward	CTGGGAAACGGGTTGAGTAA	1672 to 1691
Reverse	TACCACAGCCTTCCCAAATC	1872 to 1853
Rat *sod2* off-target		
Forward	CGCGGTGTCGGTGGCATGA	175 to 193
Reverse	CCCCTGCATCGAAACAGACTTCCG	488 to 465
Bovine *sod2* promoter		
Forward	GAGCCGTACCATCTCTTTCG	−345 to −326
Reverse	CTTCCAACTCCGGGGAAAT	−135 to −153
Bovine *sod2* enhancer		
Forward	AGCCTGTGTATGCAACCATCT	4905 to 4925
Reverse	CCCCAAATTATGTGTCCCAG	5118 to 5099
Bovine β-actin promoter		
Forward	CAGGGCGGCCAACGCCAAAA	−251 to −232
Reverse	CGAGAGGCCTGTGCTAGCGG	+41 to +22

For TaqMan primers, gene bank accession numbers for rat *SUV420h2*, *sod2*, and *β-actin* are NM_001107475.1, NM_017051.2, NM_031144.2, and for bovine *SUV420h2*, *sod2*, and *18S* are XM_598002, NM_201527.2, and X03205.1, respectively.

each immunoprecipitate were normalized to the Ct value from the input sample using the ΔΔCt method. Relative fold-changes were calculated by setting the mean fraction of normal rats as 1. For quantifying the gene expressions of *SUV420h2* and *sod2*, TaqMan primers were used. Each sample was measured in triplicate. Fold-change in mRNA abundance was calculated with the ΔΔCt method as routinely used by us (22,23).

Western blotting. Chromatin pellets or retinal homogenate were boiled for 5 to 10 min in SDS-PAGE sample buffer, and separated on a 4–20% gradient polyacrylamide gel. The proteins blotted onto membranes were blocked and incubated with the primary antibody against acetyl H3K9, or mono-, di-, or trimethyl H4K20 (H4K20me1, me2, and me3, respectively), or SUV420h2 (Abcam). After enhancing the target proteins with enhanced chemiluminescence reagent (Thermo Scientific, Rockford, IL), they were determined by autoradiography. The membranes were reprobed with normal rabbit IgG or β-actin (Sigma-Aldrich, St. Louis, MO) or histone H4 (Cell Signaling, Danvers, MA). The band intensity was quantified using Un-Scan-It Gel digitizing software (Silk Scientific, Orem, UT), and protein expression was calculated relative to normal rabbit IgG in ChIP or β-actin or histone H4 in the same samples.

For immunoprecipitation, 100–200 μg of retinal protein was incubated overnight with 1 μg antibody against NF-κB p65 or H4K20me3. The antibody-protein complex was collected with Protein A/G Plus-agarose (Santa Cruz Biotechnology) and separated on a 4–20% gradient gel. The membranes were probed for H4K20me3 or acetyl H3K9, and NF-κB p65 or H4K20me3 served as loading controls for their respective membranes. The precipitate obtained from normal rabbit IgG (Abcam) served as the negative control.

Statistical analysis. Results are presented as mean ± SD, and analyzed using the nonparametric Kruskal-Wallis test, followed by the Mann-Whitney test for multiple group comparison. Similar conclusions were achieved by using ANOVA with Fisher or Tukey tests. $P < 0.05$ is considered as significant.

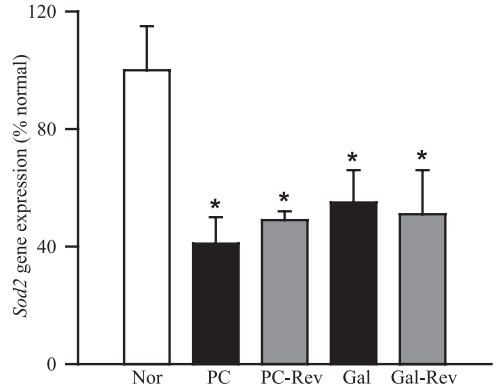

FIG. 1. Gene expression of *sod2* in rat retina. RNA was isolated from the retina using TRIzol reagent, and 1 μg RNA was converted to single-stranded cDNA and quantified spectrophotometerically. Gene expression was measured in a 90-ng cDNA template using the ABI-7500 sequence detection system. Each sample was analyzed in triplicate, and the data were normalized to β-actin expression in each sample. Fold-change relative to age-matched normal rats was calculated using the ΔΔCt method. Results are from five or more rats in each group and are represented as mean ± SD. *$P < 0.05$ compared with normal. Nor, normal.

RESULTS

Severity of hyperglycemia in rats. The body weights of the rats in the PC group were significantly lower, and their GHb values were more than twofold higher compared with the age-matched normal control rats (317 ± 32 vs. 439 ± 68 g and 12.3 ± 2.0 vs. 5.9 ± 0.9%, respectively). The rats in the GC group had body weight and GHb values (445 ± 14 g and 7.0 ± 0.4%, respectively) that were similar to the normal rats ($P > 0.05$). In PC-Rev group, the body weights and GHb levels before initiation of good glycemic control were not different from the rats in the PC group (272 ± 30 g and 11.8 ± 2.0%, respectively). However, after initiation of good control, the values became similar to those in the normal group (395 ± 35 g and 6.9 ± 0.3%). The GHb value in the Galac group was slightly higher than in the normal group (~8%), but was significantly lower than in the PC group ($P < 0.05$). The average body weights of the Galac group were ~400 g, and became similar to the normal rats after termination of the galactose diet (447 ± 21 g, GHb 6.1 ± 0.3%).

Effect of hyperglycemia on epigenetic modification of *sod2*. Diabetes inhibited the activity of retinal MnSOD (1) and also decreased its gene transcripts by 60% (Fig. 1). H4K20me3 and acetyl H3K9 were elevated by 6–11-fold at both the promoter and the enhancer of *sod2* (Fig. 2*A* and *B*). Because H4K20me3 was increased at *sod2*, the protein levels of H4K20me1, -me2, and -me3 were also quantified. As shown in Fig. 2*C*, methylation of H4K20 was increased in diabetes, and the increase in H4K20me2 and -me3 was significantly higher than that in H4K20me1. Gene and protein expressions of SUV420h2, the enzyme with dynamic functions for di- and trimethylation (16,27), were significantly elevated (Fig. 2*D* and *E*). In the same retina samples, although NF-κB p65 was elevated by more than 10-fold at both the promoter and enhancer of *sod2* (Fig. 3*A*), p50 was elevated only at its enhancer (Fig. 3*B*).

To verify the specificity of the proteins binding to the promoter and enhancer of *sod2*, the same ChIP DNA from normal rats was amplified using an off-target primer (amplified from +175 to +488 of *sod2*) by semiquantitative PCR (Fig. 3*C*) and confirmed by q-PCR (Fig. 3*D*). As shown in Fig. 3*C* and *D*, despite substantially enriched H4K20me3, acetyl H3K9, and NF-κB p65 at the promoter of *sod2*, off-target region existing in input and genomic DNA was not occupied by them and nonspecific precipitate by normal IgG was almost undetectable. H4K20me3 and acetyl H3K9 proteins, co-immunoprecipitated with p65 in chromatin, were significantly increased (Fig. 4*A*).

To verify interaction of H4K20me3 or acetyl H3K9 with NF-κB p65, retinal homogenate was immunoprecipitated with NF-κB p65 or H4K20me3 antibodies. Figure 4*B* shows that diabetes significantly increased the interaction of H4K20me3 or acetyl H3K9 with NF-κB p65. Owing to the increased expression of retinal NF-κB p65 in the PC and PC-Rev groups compared with normal (consistent with our previous results showing the activation of retinal NF-κB p65 in diabetes [12]), despite much higher interactions depicted in the Western blots, the accompanying histogram shows about a twofold increase in the ratio. However, retinal protein precipitated with rabbit IgG (negative control) yielded negligible expressions of H4K20me3 or acetyl H3K9 (Fig. 4*C*). In addition, as shown in Fig. 4*D*, in the same animals, diabetes also increased the interaction of H4K20me3 and acetyl H3K9.

As with diabetes, gene expression of retinal *sod2* were significantly reduced in the retina obtained from experimentally galactosemic rats, and H4K20me3 and acetylated H3K9 at both the promoter and enhancer of *sod2* were elevated (Fig. 2). This was accompanied by concomitant increases of p65 and p50 at the enhancer of *sod2*, and only p65 at the promoter of *sod2* ($P < 0.05$ compared with normal, Fig. 3).

Reversal of hyperglycemia and retinal *sod2*. Reinstitution of good glycemic control for 2 months after 2 months of poor glycemic control (PC-Rev) failed to provide any benefit to retinal *sod2* (Fig. 1). It had no significant effect on retinal H4K20me3 and acetyl H3K9 at the promoter and enhancer of *sod2*, and *SUV420h2* expression remained elevated (Fig. 2). The diabetes-induced increase

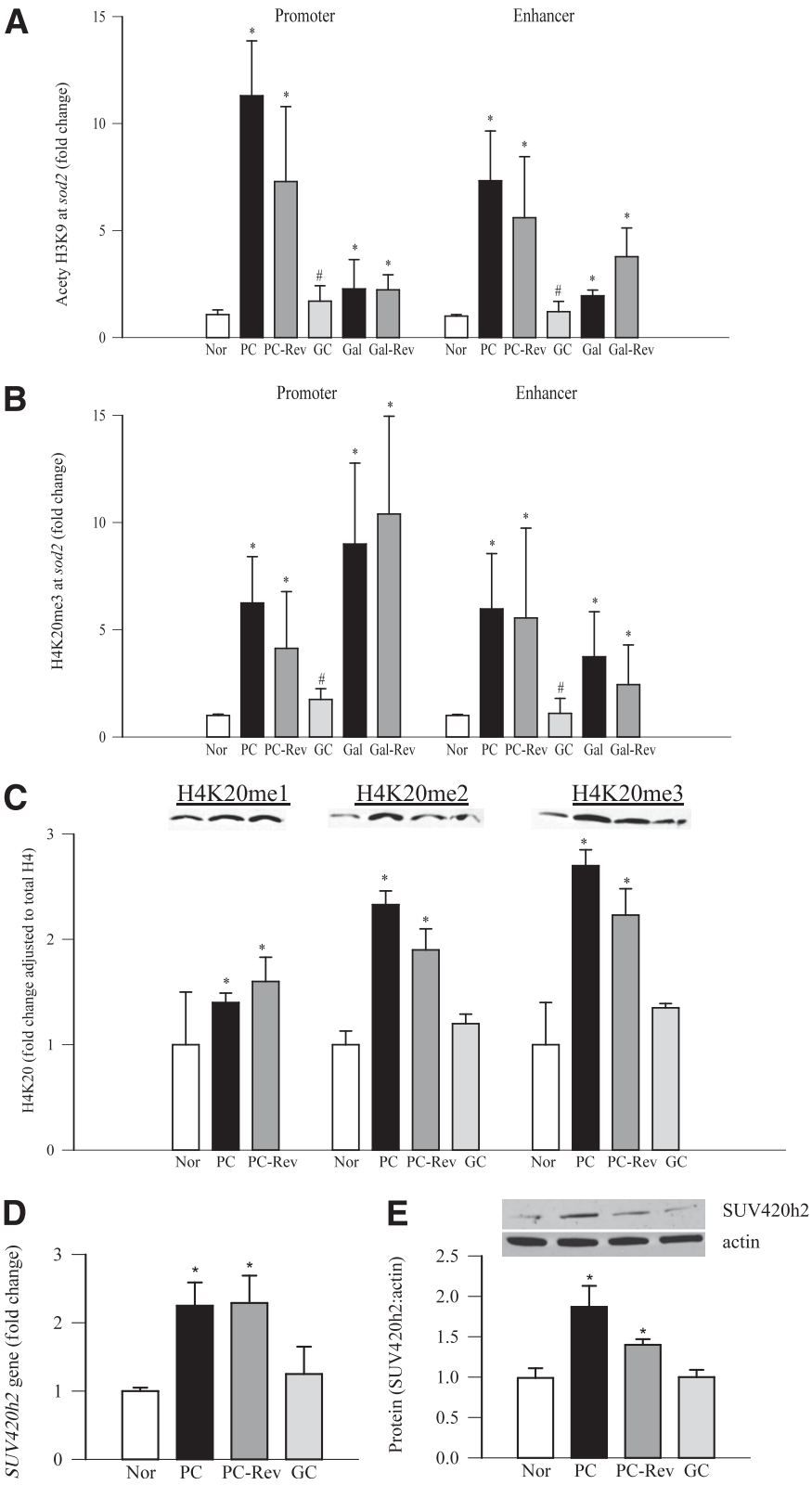

FIG. 2. Retinal H4K20me3 and acetyl H3K9 at *sod2*, methylation of H4K20, and the expression of SUV420h2: the levels of acetyl H3K9 (*A*) and H4K20me3 (*B*) at the *sod2* promoter and enhancer were determined using the ChIP technique. Retinal chromatins were immunoprecipitated with H4K20me3 or acetyl H3K9 antibody, and the *sod2* promoter and enhancer region were amplified. The q-PCR value in each immunoprecipitate was normalized to the Ct value from the input sample using the ΔΔCt method. *C*: The protein expression of methylated H4K20 was detected by Western blot technique using antibodies specific for mono-, di-, and trimethyl H4K20 using histone H4 as the loading control. *D*: Gene expression of *SUV420h2* was detected by q-PCR and analyzed by the ΔΔCt method. The housekeeping gene was β-actin. Fold-changes were calculated by setting the mean fraction of normal rats as 1. *E*: Protein expression of SUV420h2 was quantified by Western blot, and β-actin was used as a loading protein. Values are represented as mean ± SD of five to six rats in each group. *$P < 0.05$ compared with normal, and #$P < 0.05$ compared with PC. Nor, normal.

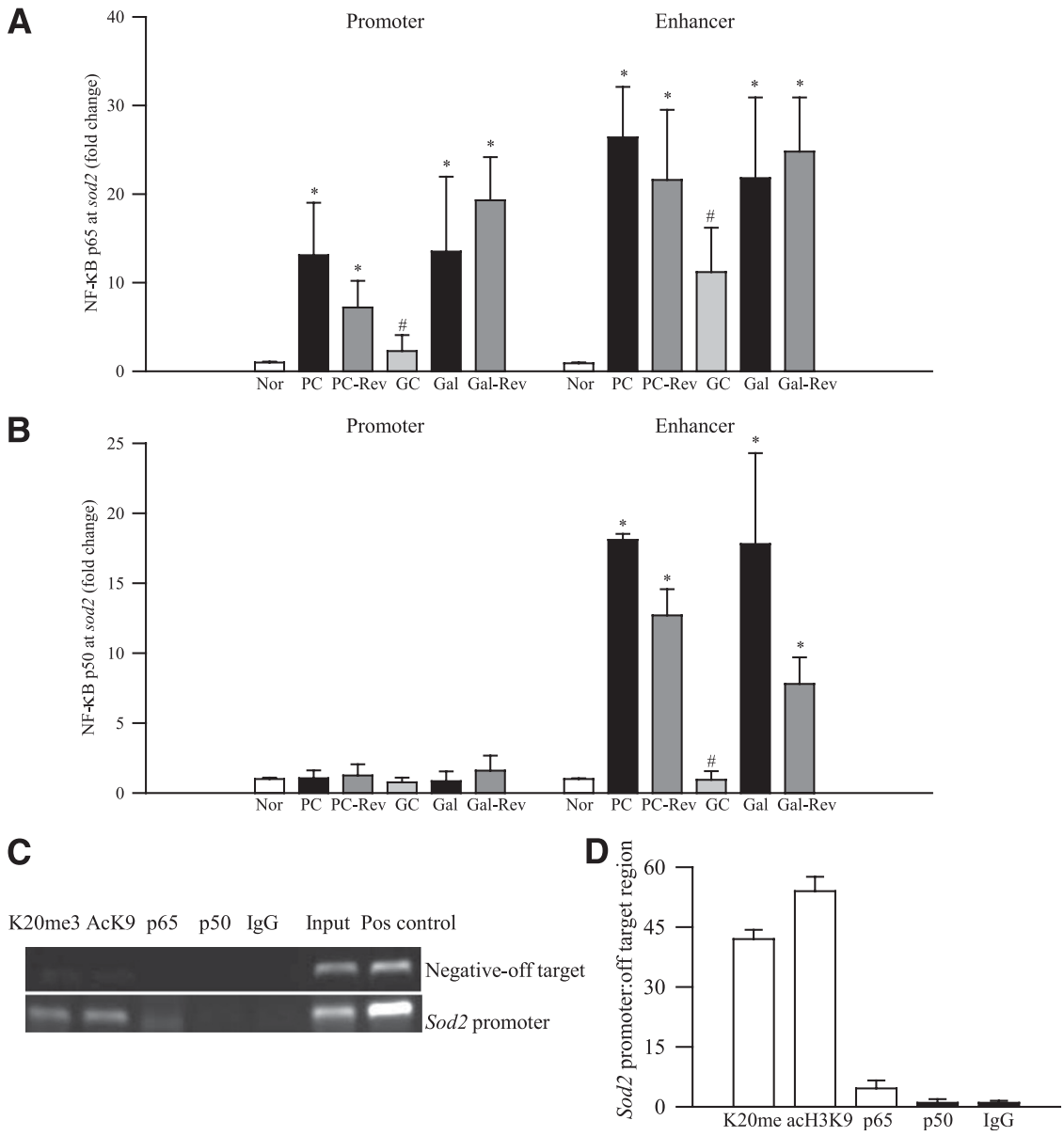

FIG. 3. NF-κB p65 and NF-κB p50 in retinal *sod2*, and the specificity of the ChIP assay. The levels of retinal NF-κB p65 (*A*) and NF-κB p50 (*B*) at the *sod2* promoter and enhancer were determined by ChIP. Fold enrichment of NF-κB p65 or p50 was compared with the values obtained from the age-matched normal rats, which were set as 1. The specificity of the ChIP assay was verified by using an off-target primer by semiquantitative PCR (*C*), and confirmed by SYBER green-based real-time q-PCR (*D*). Immunoprecipitated DNA from normal retina was amplified using a primer specific to an off-target region (+175 to +488) or to the promoter (−529 to −282) region on *sod2*. The total genomic DNA obtained from the retina of normal rats served as the positive DNA control. Each measurement was made in the retina obtained from five to seven rats in each group. K20me3 and AcK9, ChIP with H4K20me3 and acetyl H3K9, respectively; p65 and p50, ChIP with NF-κB p65 and p50, respectively; IgG, ChIP with normal IgG; input, sample without ChIP; and pos control, positive control of genomic DNA. *$P < 0.05$ compared with normal and #$P < 0.05$ compared with PC. ac, acetyl; Nor, normal.

in p65 at the promoter and enhancer of *sod2*, and H4K20me3 and acetyl H3K9 proteins co-immunoprecipitated with p65 in chromatin, and also in retinal homogenate, remained significantly elevated ($P > 0.05$ compared with PC, Figs. 3 and 4). The levels of H4K20me1, -me2, and -me3, and the expression of SUV420h2 remained elevated (Fig. 2*C–E*). In concert, termination of experimental galactosemia (Galac-Rev) also failed to prevent elevations in H4K20me3, acetyl H3K9, and p65 at the promoter and enhancer of *sod2* (Figs. 2 and 3).

Effect of continuous good glycemic control on epigenetic modification of retinal *sod2*. In contrast, when good glycemic control was instituted immediately after induction of diabetes in rats (GC group), values for retinal H4K20me3, acetyl H3K9, and NF-κB p50 were significantly different from those obtained from the rats in PC or Galac groups. Although p65 at the enhancer and promoter of *sod2* was slightly higher than observed in normal rats, the values remained significantly different from those obtained from rats in the PC or PC-Rev groups ($P < 0.05$, Figs. 2 and 3). The levels of methylated H4K20me2 and -me3, and SUV420h2 were not different from those obtained from normal rats (Fig. 2*C–E*). Similarly, the values for H4K20me3 and acetyl H3K9 proteins, co-immunoprecipitated with NF-κB p65 in chromatin, were also lower than those observed in the PC group (Fig. 4*A*).

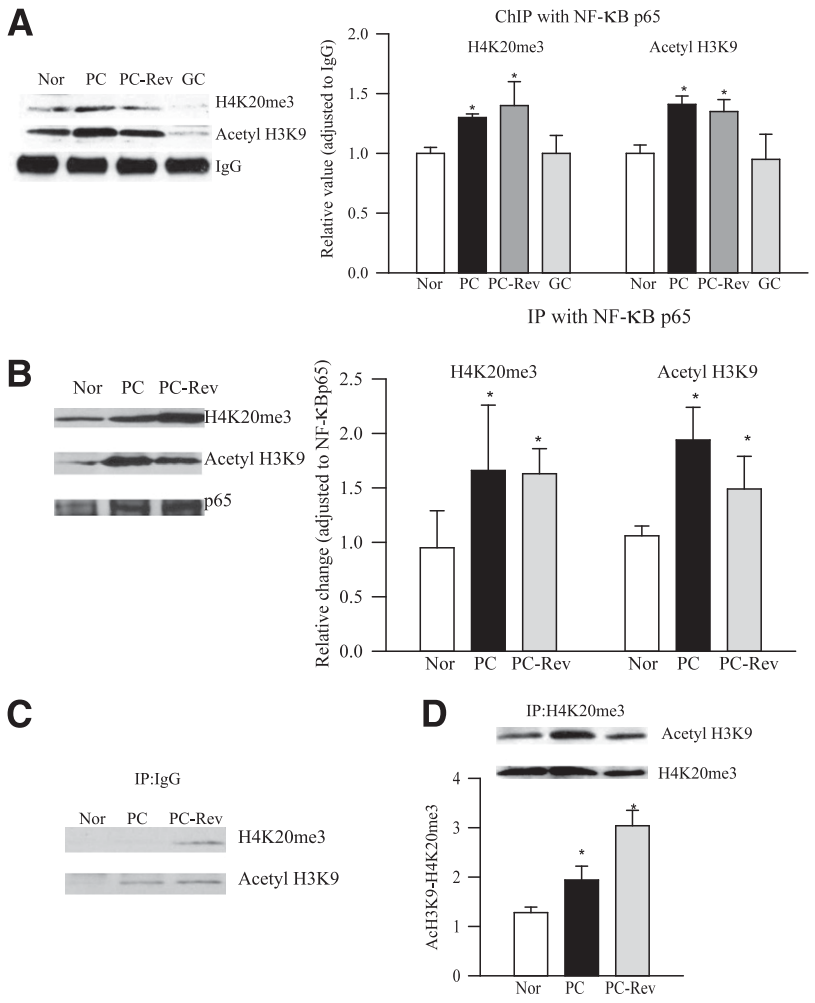

FIG. 4. The interactions of H4K20me3 and acetyl H3K9 with NF-κB p65 in the retina. *A*: The crosslinked retina was immunoprecipitated with NF-κB p65 antibody, and the pull-down proteins in the immunoprecipitated chromatin were separated by Western blots using acetyl H3K9 and H4K20me3 antibodies. IgG was used as a loading control. The histogram (*upper right*) represents the intensity of each band adjusted to IgG in the same sample. *B*: The interaction of NF-κB p65 with acetyl H3K9 or H4K20me3 was detected by immunoprecipitation. Rat retinal homogenate was immunoprecipitated with NF-κB p65 antibody. Acetyl H3K9 or H4K20me3 in the precipitate was detected by Western blot. For loading efficiency, the membranes were reprobed with NF-κB p65. The histograms represent the ratio of NF-κB p65/acetyl H3K9 or NF-κB p65/H4K20me3 adjusted to p65 in each lane. *C*: Expressions of H4K20me3 or acetyl H3K9 in retinal protein precipitated with rabbit IgG (negative control for IP). *D*: For H4K20me3 and acetyl H3K9 interactions, rat retinal homogenate was immunoprecipitated with H4K20me3 antibody, and the immunoprecipitate was detected for acetyl H3K9 by Western blot. The values represent mean ± SD obtained from four to five rats in each group. *$P < 0.05$ compared with normal. Ac, acetyl; IP, immunoprecipitation; Nor, normal.

Epigenetic regulation of *sod2* in isolated retinal endothelial cells. High glucose (20 mmol/L) exposure of retinal endothelial cells significantly decreased the gene expression of *sod2* ($P < 0.05$, Fig. 5*A*), increased the gene expression (Fig. 5*B*) and protein levels (Fig. 5*C*) of SUV420h2, and elevated H4K20me3 and acetyl H3K9 at the promoter and enhancer of *sod2* compared with the values obtained from the cells incubated in normal glucose (Fig. 6*A* and *B*). These changes were not due to increased osmolarity experienced by the cells in a high glucose medium because the addition of 20 mmol/L mannitol instead of 20 mmol/L glucose failed to produce any effect on *SUV420h2* gene expression and the enrichment of H4K20me3 and acetyl H3K9 at *sod2* (Figs. 5*B*, 6*A* and *B*).

Figure 6*B* and *C* shows that glucose exposure increased acetyl H3K9 at the *sod2* promoter, but the negative antibody control, IgG, produced almost negligible PCR products for the *sod2* promoter, and the yield of ChIP IgG was less than 2% of the product from ChIP with the acetyl H3K9 antibody. In addition, the amplification of TFIIB (positive control) at the β-actin promoter was similar in low and high glucose conditions (Fig. 6*C*). The increased *SUV420h2* gene expression and the enrichment of H4K20me3 and acetyl H3K9 at *sod2* persisted even when 4 days of high glucose was followed by 4 days of normal glucose exposure (20-5 group).

Because hyperglycemia increases oxidative stress, and oxidative stress can result in epigenetic modifications, we investigated the effect of *sod2* overexpression. Figure 6*A* shows that overexpression of *sod2* successfully blocked the increase of H4K20me3 at the *sod2* promoter and enhancer. To further evaluate the effects of H4K20me3 and NF-κB p65 on the expression of *sod2*, *SUV420h2* or NF-κB p65 were inhibited by their respective siRNAs. Figure 5*B* and *C* shows that high glucose increased the gene and protein expressions of SUV420h2, and this was successfully prevented by siRNA-*SUV420h2*. Transfection with siRNA-*SUV420h2* also prevented an increase in H4K20me3 at the *sod2* enhancer and ameliorated a decrease in *sod2* mRNA (Figs. 5 and 7). In addition, transfection of cells with

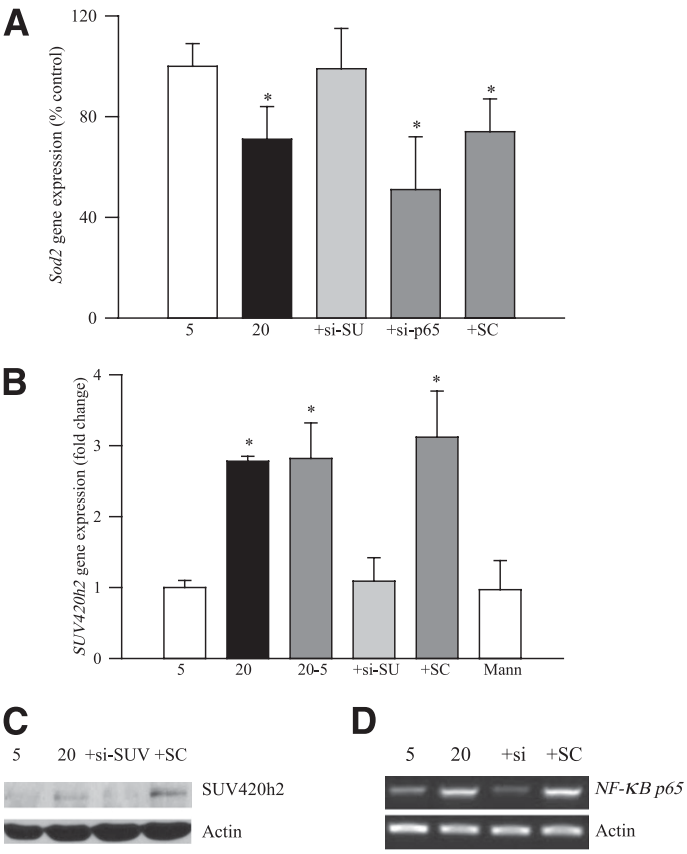

FIG. 5. Gene expression of *sod2*, *SUV420h2*, and *NF-κB p65* in retinal endothelial cells. Gene expressions of *sod2* (*A*) and *SUV420h2* (*B*) and protein expression of SUV420h2 (*C*) were evaluated in retinal endothelial cells. *D*: The efficiency of *NF-κB p65*–siRNA on p65 gene expression was measured by semiquantitative PCR. 5 and 20, cells incubated in 5 mmol/L glucose or 20 mmol/L glucose; +siSU, +si-p65, or SC, cells transfected with siRNA-*SUV420h2* or siRNA–*NF-κB p65*, or scrambled RNA, respectively, followed by incubation in 20 mmol/L glucose for 4 days; and Mann, cells incubated in 20 mmol/L mannitol instead of 20 mmol/L glucose. The values represent mean ± SD obtained from four to five different experiments, and the Western blot (*C*) is representative of three different experiments. *$P < 0.05$ compared with the values obtained from the cells incubated in 5 mmol/L glucose.

siRNA–*NF-κB*, which inhibited glucose-induced increase in p65 (Fig. 5*D*), further downregulated *sod2* gene expression (Fig. 5*A*).

DISCUSSION

The mitochondrial superoxide scavenging enzyme, MnSOD, has an important role in protecting mitochondria from oxidative damage. Overexpression of *sod2* in diabetes protects retinal mitochondrial DNA damage (23) and prevents the development of retinopathy (3). The enzyme activity continues to be compromised after reinstitution of normal glycemic control in diabetic rats, suggesting it is important in the metabolic memory phenomenon (7). This study provides novel data showing diabetes-induced epigenetic regulation of retinal *sod2* and increased H4K20me3, acetyl H3K9, and NF-κB p65 at its promoter/enhancer. Increased acetyl H3K9 and NF-κB p65 at the promoter/enhancer of *sod2* interacts with H4K20me3, suggesting a loss of their activation function. Furthermore, reinstitution of good control for 2 months after 2 months of hyperglycemia has no beneficial effect on increased methylation of H4K20 and acetylation of H3K9 and p65 at the promoter/enhancer of *sod2*, suggesting the role of epigenetic modifications of *sod2* in the metabolic memory phenomenon associated with the progression of diabetic retinopathy.

Histone modifications regulate gene expression, acetyl H3K9 is considered to open up the chromatin (15), and H4K20me3, a modification with more general function in chromatin management, compacts it and inhibits genes by blocking the access of other transcription regulators to the genes (28,29). In cancer cells, decreased acetyl H3K9 at the promoter and enhancer of *sod2* is associated with decreased *sod2* (30). In diabetes, despite decreased activity of retinal MnSOD (7) and reduced transcripts, we show that acetyl H3K9 and H4K20me3 are both increased at the promoter and enhancer of *sod2*. In support, multiple histone modifications can act concurrently to specify distinct chromatin structure, and modifications for activation and repression may bind to the same gene simultaneously, suggesting a bivalent domain. The coexistence of H3K4me3 (activator) and H3K27me3 (repressor), in addition to downregulating genes can also activate them, and the same lysine residue can be methylated to different degrees with different functional consequences (31). Furthermore, we cannot rule out the possibility that increased acetyl H3K9, despite decreased *sod2* transcript, could be due to an interaction of H4K20me3 with acetyl H3K9 that abolishes the activation function of acetyl H3K9.

The transcription-initiation site of *sod2* is preceded by a promoter with the enhancer elements located in the second intron containing multiple potential regulatory elements, including several SP1 sites, two NF-κB sites, and an antioxidant-response element (32). Homodimer and heterodimer units of NF-κB bind to DNA binding sites with different affinities within the target genes (14). NF-κB p65/p50 binds to the enhancer and is important for cytokine-induced *sod2*, and also, the binding of NF-κB p65/p50 to the *sod2* promoter is associated with its activation (30). In contrast, p50/p50 represses *sod2* by competing with p65/p50 to the enhancer of *sod2*. Sp1 at the promoter and NF-κB at the enhancer are integrated by a connection protein, nucleophosmin, which binds to an 11-G single-strand loop structure in the *sod2* promoter (13,14,33), suggesting strong interactions among various regulators of *sod2*. NF-κB acts as a proapoptotic factor, and the expressions of the p65 and p50 subunits are elevated in the retina in diabetes (12,34,35). We show that hyperglycemia increases p65 at both promoter and enhancer, and p50 only at the enhancer of *sod2*, and that genetic manipulation of p65 (siRNA) in retinal endothelial cells further decreases *sod2* transcripts, supporting the role of activation of p65 at *sod2*.

In addition, our results show that the p65 subunit of NF-κB also interacts with H4K20me3, raising the possibility that this interaction could contribute to the decreased MnSOD activity in diabetes and that the binding of H4K20me3 in *sod2* may facilitate the recruitment of p50 to its enhancer, decreasing the transcription. In support, epigenetic modifications are postulated in altering gene expression patterns associated with various diseases, including diabetes (17,36–38).

Reinstitution of normal glycemic control for 2 months after 2 months of hyperglycemia failed to normalize the increased H4K20me3, p50, p65, and acetyl H3K9 at *sod2*, and *sod2* gene expression continued to be subnormal. The persistent epigenetic regulation of retinal *sod2* in the

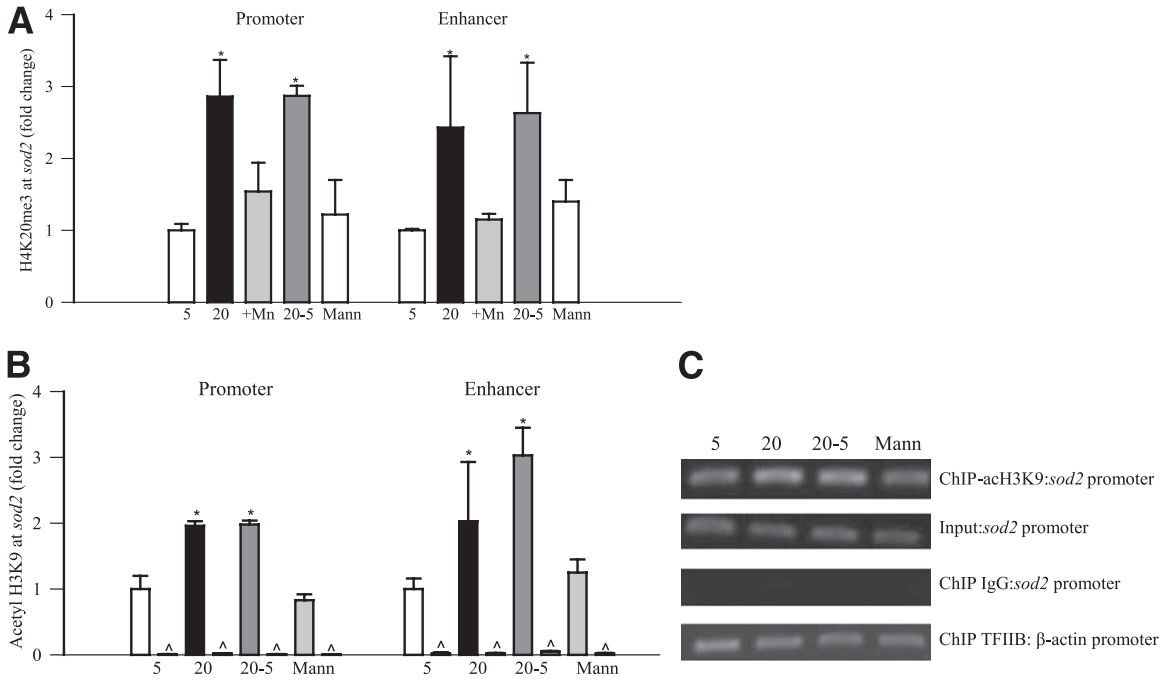

FIG. 6. H4K20me3 and acetyl H3K9 at *sod2*, and evaluation of ChIP controls in retinal endothelial cells. *A* and *B*: H4K20me3 and acetyl H3K9 at the *sod2* promoter and enhancer were measured by ChIP assay with SYBR green-based real-time q-PCR. Rabbit IgG served as a negative antibody control (indicated as ^). *C*: ChIP controls were verified by PCR. Crosslinked cells were immunoprecipitated with acetyl H3K9 or TFIIB antibody or normal rabbit IgG. The *sod2* promoter occupied by acetyl H3K9 and the β-actin promoter occupied by TFIIB were amplified in purified ChIP-DNA. For the ChIP assay, the positive and negative controls were β-actin promoter occupied by TFIIB and the *sod2* promoter occupied by IgG, respectively. The internal control included the input. 5 and 20, cells incubated in 5 mmol/L glucose or 20 mmol/L glucose; +Mn, cells transfected with *sod2* plasmid, followed incubation in 20 mmol/L glucose for 4 days; and Mann, cells incubated in 20 mmol/L mannitol instead of 20 mmol/L glucose. *$P < 0.05$ compared with the values obtained from the cells incubated in 5 mmol/L glucose. ac, acetyl.

normal glycemic state after a period of hyperglycemia is consistent with the results showing persistent epigenetic regulation of NF-κB in aortic cells (17,24). Here we show that hyperglycemia increases SUV420h2 and methylation of H4K20, and reversal of hyperglycemia fails to normalize it. This could be due to regulation of histone modification by increased oxidative stress experienced by the retina in diabetes, and once these modifications are formed, they are inherited by the next cell cycle independent of the actual glycemia (17,24,36–38). In support, our recent study demonstrated a significant role of histone acetylation in the development of diabetic retinopathy and in the metabolic memory phenomenon (25), and others have shown that short-term hyperglycemia, followed by normal glucose, have sustained an increase in H3K4me1 and a decrease in H3K9me3 at the promoter of p65 (24,36–38). The possibility that the increased NF-κB p65 at *sod2* promoter might be due to increased levels of p65 in hyperglycemic milieu cannot be ruled out.

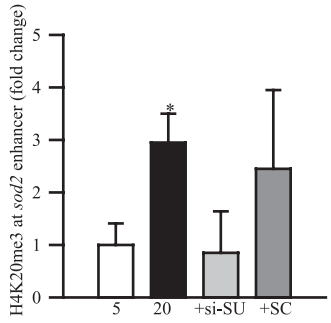

FIG. 7. Effect of siRNA-*SUV420h2* on H4K20me3 at *sod2* enhancer. The effect of siRNA-*SUV420h2* on the enrichment of H4K20me3 at the *sod2* enhancer was determined by chromatin immunoprecipitating the cells with H4K20me3 antibody. The *sod2* enhancer was measured by q-PCR. 5 and 20, cells incubated in 5 mmol/L glucose or 20 mmol/L glucose for 4 days, respectively; +si-SU, +SC, cells transfected with siRNA-*SUV420h2* or scrambled RNA, respectively, followed by incubation in 20 mmol/L glucose for 4 days. The values are represented as mean ± SD obtained from four to five different experiments. *$P < 0.05$ compared with the values obtained from the cells incubated in 5 mmol/L glucose.

The retina is a complex tissue with multiple layers and cell types, and capillary cells are the major targets of the

Good glycemic control, if initiated soon after the induction of diabetes, protected epigenetic changes in retinal *sod2*. This is consistent with our previous results that show that if the rats are maintained in good glycemic control immediately after the induction of diabetes, the retina escapes from increased oxidative stress and nitrotyrosine accumulation (7,19) and imply that the epigenetic modifications observed in PC-Rev group during good glycemic control are not influenced by high insulin administered to maintain such glycemic control. This further strengthens the importance of early and sustained good glycemic control for diabetic patients.

Experimentally, galactosemic rats do not experience insulin deficiency or lipid/protein dysmetabolism but present retinal histopathology similar to that observed in diabetic rats (39). Similar epigenetic modifications in galactosemic animals strongly imply that hyperglycemic insult is sufficient to initiate epigenetic modifications of retinal *sod2* and that the process continues even after the insult is halted.

histopathology characteristic of diabetic retinopathy (40). Results from our laboratory and others have shown that retinal capillary cells incubated in high glucose show similar abnormalities as those observed in the retina in diabetes, and these cells present similar metabolic memory phenomenon as observed in the retina from diabetic rodents (9,12,21,23,41–46). The active p65 subunit of NF-κB is linked with persisting epigenetic changes in aortic endothelial cells, and these changes are maintained even hyperglycemia is removed (17). We show that genetic manipulation of *SUV420h2* prevents a glucose-induced increase in H4K20me3 at the *sod2* enhancer and a decrease in *sod2* transcript, and overexpression of *sod2* prevents an increase in H4K20me3 at *sod2*. This suggests that epigenetic regulations of *sod2* and SUV420h2 are under the control of superoxide radicals. Failure of these modifications to reverse after termination of hyperglycemia further confirms the role of *sod2* epigenetic modifications in the development of diabetic retinopathy and the metabolic memory phenomenon.

The retina and its capillary cells experience mitochondrial dysfunction in diabetes, and the pathogenic mechanisms that are postulated in the development of complications have a single unifying process—superoxide production from the mitochondria (47). In rodent models, compromised MnSOD activity and mitochondrial dysfunction precede the development of diabetic retinopathy (1,3,8,48), and the mitochondria remain dysfunctional when the histopathology is seen in the retinal vasculature (3,4,7). Overexpression of *sod2* protects mitochondrial DNA from being damaged and the retinal vasculature from the pathology (6,8,9,23), suggesting a major role of MnSOD in the development of diabetic retinopathy. Thus, the significance of epigenetic regulation of *sod2*, observed in the current study in the retina and in its capillary cells, further supports its contributions in the development and progression of diabetic retinopathy.

Histone modifications influence the overall chromatin structure and result in functional consequences in cellular processes, and methylation of H4K20 has been implicated in DNA damage, chromatin maintenance, and transcriptional repression. Although H4K20me1 is associated with cell cycle regulation, H4K20me3 is associated with cancers and aging (49,50). Our data demonstrate that diabetes increases total retinal H4K20 methylation, and increases in H4K20me2 and H4K20me3 are significantly greater compared with H4K20me1. Reversal of hyperglycemia fails to provide any benefit. Furthermore, we show that, SUV420h2, an enzyme important for di- and trimethylation, is increased, and that inhibition of SUV420h2 prevents H4K20me3 at the *sod2* enhancer and ameliorates a decrease in *sod2* gene expression. However, others have shown glucose-induced monomethylation of H3K4 by Set7 in aortic endothelial cells is associated with the transcription activation and regulation of NF-κB and is important in the sustained increase in the NF-κB p65 gene (17,24,37). Our data showing a sustained increase of SUV420h2 in the retina and its capillary cells in hyperglycemia, and prevention of H4K20me3 at *sod2* by its siRNA, strongly suggest SUV420h2 is important in the metabolic memory phenomenon associated with diabetic retinopathy. We cannot, however, rule out the regulation of retinal *sod2* by other histone and nonhistone modifications, including methylation of H3K9 and activation of Set7/9.

In conclusion, this is the first report showing that retinal *sod2* is epigenetically regulated in diabetes and that these modifications continue after termination of hyperglycemia, suggesting their role in the metabolic memory phenomenon associated with the continued progression of diabetic retinopathy. Modulation of epigenetic changes by pharmaceutical or molecular means may provide a potential strategy to retard the development/progression of diabetic retinopathy.

ACKNOWLEDGMENTS

This study was partly supported by grants from the National Institutes of Health, Juvenile Diabetes Research Foundation, the Thomas Foundation, and Research to Prevent Blindness.

No potential conflicts of interest relevant to this article were reported.

Q.Z. researched data and wrote the manuscript. R.A.K. wrote the manuscript and reviewed and edited the manuscript.

The authors appreciate the technical assistance of Mamta Kanwar, Yakov Shamailov, and Dr. Julia Santos, Wayne State University, for help with PCR.

REFERENCES

1. Kowluru RA, Kern TS, Engerman RL. Abnormalities of retinal metabolism in diabetes or experimental galactosemia. IV. Antioxidant defense system. Free Radic Biol Med 1997;22:587–592
2. Du Y, Miller CM, Kern TS. Hyperglycemia increases mitochondrial superoxide in retina and retinal cells. Free Radic Biol Med 2003;35:1491–1499
3. Kanwar M, Chan PS, Kern TS, Kowluru RA. Oxidative damage in the retinal mitochondria of diabetic mice: possible protection by superoxide dismutase. Invest Ophthalmol Vis Sci 2007;48:3805–3811
4. Mizutani M, Kern TS, Lorenzi M. Accelerated death of retinal microvascular cells in human and experimental diabetic retinopathy. J Clin Invest 1996;97:2883–2890
5. Kern TS, Tang J, Mizutani M, et al. Response of capillary cell death to aminoguanidine predicts the development of retinopathy: comparison of diabetes and galactosemia. Invest Ophthalmol Vis Sci 2000;41:3972–3978
6. Kowluru RA, Odenbach S. Effect of long-term administration of alpha-lipoic acid on retinal capillary cell death and the development of retinopathy in diabetic rats. Diabetes 2004;53:3233–3238
7. Kowluru RA, Kanwar M, Kennedy A. Metabolic memory phenomenon and accumulation of peroxynitrite in retinal capillaries. Exp Diabetes Res 2007;2007:21976
8. Kowluru RA, Kowluru V, Xiong Y, Ho YS. Overexpression of mitochondrial superoxide dismutase in mice protects the retina from diabetes-induced oxidative stress. Free Radic Biol Med 2006;41:1191–1196
9. Kowluru RA, Atasi L, Ho YS. Role of mitochondrial superoxide dismutase in the development of diabetic retinopathy. Invest Ophthalmol Vis Sci 2006;47:1594–1599
10. Kuo S, Chesrown SE, Mellott JK, Rogers RJ, Hsu JL, Nick HS. In vivo architecture of the manganese superoxide dismutase promoter. J Biol Chem 1999;274:3345–3354
11. Rogers RJ, Chesrown SE, Kuo S, Monnier JM, Nick HS. Cytokine-inducible enhancer with promoter activity in both the rat and human manganese-superoxide dismutase genes. Biochem J 2000;347:233–242
12. Kowluru RA, Chakrabarti S, Chen S. Re-institution of good metabolic control in diabetic rats on the activation of caspase-3 and nuclear transcriptional factor (NF-kB) in the retina. Acta Diabetol 2004;44:194–199
13. Guo Z, Boekhoudt GH, Boss JM. Role of the intronic enhancer in tumor necrosis factor-mediated induction of manganous superoxide dismutase. J Biol Chem 2003;278:23570–23578
14. Dhar SK, Xu Y, Noel T, St Clair DK. Chronic exposure to 12-O-tetradecanoylphorbol-13-acetate represses sod2 induction in vivo: the negative role of p50. Carcinogenesis 2007;28:2605–2613
15. Fuchs J, Demidov D, Houben A, Schubert I. Chromosomal histone modification patterns—from conservation to diversity. Trends Plant Sci 2006;11:199–208
16. Benetti R, Gonzalo S, Jaco I, et al. Suv4-20h deficiency results in telomere elongation and derepression of telomere recombination. J Cell Biol 2007;178:925–936

17. Brasacchio D, Okabe J, Tikellis C, et al. Hyperglycemia induces a dynamic cooperativity of histone methylase and demethylase enzymes associated with gene-activating epigenetic marks that coexist on the lysine tail. Diabetes 2009;58:1229–1236
18. Writing Team for the Diabetes Control and Complications Trial/Epidemiology of Diabetes Interventions and Complications Research Group. Sustained effect of intensive treatment of type 1 diabetes mellitus on development and progression of diabetic nephropathy: the Epidemiology of Diabetes Interventions and Complications (EDIC) study. JAMA 2003;290:2159–2167
19. Kowluru RA. Effect of reinstitution of good glycemic control on retinal oxidative stress and nitrative stress in diabetic rats. Diabetes 2003;52:818–823
20. Kanwar M, Kowluru RA. Role of glyceraldehyde 3-phosphate dehydrogenase in the development and progression of diabetic retinopathy. Diabetes 2009;58:227–234
21. Kowluru RA, Chan PS. Metabolic memory in diabetes - from in vitro oddity to in vivo problem: role of apoptosis. Brain Res Bull 2010;81:297–302
22. Madsen-Bouterse SA, Mohammad G, Kanwar M, Kowluru RA. Role of mitochondrial DNA damage in the development of diabetic retinopathy, and the metabolic memory phenomenon associated with its progression. Antioxid Redox Signal 2010;13:797–805
23. Madsen-Bouterse SA, Zhong Q, Mohammad G, Ho YS, Kowluru RA. Oxidative damage of mitochondrial DNA in diabetes and its protection by manganese superoxide dismutase. Free Radic Res 2010;44:313–321
24. El-Osta A, Brasacchio D, Yao D, et al. Transient high glucose causes persistent epigenetic changes and altered gene expression during subsequent normoglycemia. J Exp Med 2008;205:2409–2417
25. Zhong Q, Kowluru RA. Role of histone acetylation in the development of diabetic retinopathy and the metabolic memory phenomenon. J Cell Biochem 2010;110:1306–1313
26. Mohammad G, Kowluru RA. Matrix metalloproteinase-2 in the development of diabetic retinopathy and mitochondrial dysfunction. Lab Invest 2010;90:1365–1372
27. Schotta G, Lachner M, Sarma K, et al. A silencing pathway to induce H3-K9 and H4-K20 trimethylation at constitutive heterochromatin. Genes Dev 2004;18:1251–1262
28. Poleshko A, Einarson MB, Shalginskikh N, et al. Identification of a functional network of human epigenetic silencing factors. J Biol Chem 2010;285:422–433
29. Lan F, Shi Y. Epigenetic regulation: methylation of histone and non-histone proteins. Sci China C Life Sci 2009;52:311–322
30. Hitchler MJ, Oberley LW, Domann FE. Epigenetic silencing of SOD2 by histone modifications in human breast cancer cells. Free Radic Biol Med 2008;45:1573–1580
31. Bernstein BE, Mikkelsen TS, Xie X, et al. A bivalent chromatin structure marks key developmental genes in embryonic stem cells. Cell 2006;125:315–326
32. Jones PL, Kucera G, Gordon H, Boss JM. Cloning and characterization of the murine manganous superoxide dismutase-encoding gene. Gene 1995;153:155–161
33. Tong X, Yin L, Washington R, Rosenberg DW, Giardina C. The p50-p50 NF-kappaB complex as a stimulus-specific repressor of gene activation. Mol Cell Biochem 2004;265:171–183
34. Romeo G, Liu WH, Asnaghi V, Kern TS, Lorenzi M. Activation of nuclear factor-kappaB induced by diabetes and high glucose regulates a proapoptotic program in retinal pericytes. Diabetes 2002;51:2241–2248
35. Zheng L, Howell SJ, Hatala DA, Huang K, Kern TS. Salicylate-based anti-inflammatory drugs inhibit the early lesion of diabetic retinopathy. Diabetes 2007;56:337–345
36. Villeneuve LM, Reddy MA, Lanting LL, Wang M, Meng L, Natarajan R. Epigenetic histone H3 lysine 9 methylation in metabolic memory and inflammatory phenotype of vascular smooth muscle cells in diabetes. Proc Natl Acad Sci USA 2008;105:9047–9052
37. Siebel AL, Fernandez AZ, El-Osta A. Glycemic memory associated epigenetic change. Biochem Pharmacol 2010:15:1853–1859
38. Villeneuve LM, Natarajan R. The role of epigenetics in the pathology of diabetic complications. Am J Physiol Renal Physiol 2010;299:F14–F25
39. Kern TS, Engerman RL. Galactose-induced retinal microangiopathy in rats. Invest Ophthalmol Vis Sci 1995;36:490–496
40. Engerman RL, Bloodworth JMB Jr. Experimental diabetic retinopathy in dogs. Arch Ophthalmol 1965;73:205–210
41. Du Y, Sarthy VP, Kern TS. Interaction between NO and COX pathways in retinal cells exposed to elevated glucose and retina of diabetic rats. Am J Physiol Regul Integr Comp Physiol 2004;287:R735–R741
42. Kowluru RA, Abbas SN. Diabetes-induced mitochondrial dysfunction in the retina. Invest Ophthalmol Vis Sci 2003;44:5327–5334
43. Kowluru RA, Kanwar M. Oxidative stress and the development of diabetic retinopathy: contributory role of matrix metalloproteinase-2. Free Radic Biol Med 2009;46:1677–1685
44. Madsen-Bouterse S, Mohammad G, Kowluru RA. Glyceraldehyde-3-phosphate dehydrogenase in retinal microvasculature: implications for the development and progression of diabetic retinopathy. Invest Ophthalmol Vis Sci 2010;51:1765–1772
45. Ihnat MA, Thorpe JE, Kamat CD, et al. Reactive oxygen species mediate a cellular 'memory' of high glucose stress signalling. Diabetologia 2007;50:1523–1531
46. Roy S, Sala R, Cagliero E, Lorenzi M. Overexpression of fibronectin induced by diabetes or high glucose: phenomenon with a memory. Proc Natl Acad Sci USA 1990;87:404–408
47. Brownlee M. The pathobiology of diabetic complications: a unifying mechanism. Diabetes 2005;54:1615–1625
48. Kowluru RA, Tang J, Kern TS. Abnormalities of retinal metabolism in diabetes and experimental galactosemia. VII. Effect of long-term administration of antioxidants on the development of retinopathy. Diabetes 2001;50:1938–1942
49. Wang CM, Tsai SN, Yew TW, Kwan YW, Ngai SM. Identification of histone methylation multiplicities patterns in the brain of senescence-accelerated prone mouse 8. Biogerontology 2010;11:87–102
50. Wang D, Xia X, Weiss RE, Refetoff S, Yen PM. Distinct and histone-specific modifications mediate positive versus negative transcriptional regulation of TSHalpha promoter. PLoS ONE 2010;5:e9853